Environmental Science and Pollution Research (2022) 29:44693–44708
https://doi.org/10.1007/s11356-022-18744-8

RESEARCH ARTICLE

Attribution of vegetation coverage change to climate change and human activities based on the geographic detectors in the Yellow River Basin, China

Xiaojuan Deng[1,4] · Shi Hu[2] · Chesheng Zhan[3]

Received: 20 October 2021 / Accepted: 14 January 2022 / Published online: 8 February 2022

Abstract

Quantitatively, analyzing the driving mechanism of vegetation coverage change is of important significance for regional ecological environment evaluation and protection. Based on time series NDVI data and meteorological data of the Yellow River Basin (Inner Mongolia Section), the trend and significance of climate factors and vegetation coverage in the YRB (IMS) and four sub-regions (the Hetao Irrigation district, the Ten Tributaries region, the Hunhe river basin, and the Dahei river basin) from 2000 to 2018 were ascertained. We used geographic detectors to quantitatively analyze the effects of detection factors on vegetation coverage change. The results indicated that the spatial pattern of vegetation variation and climate change had obvious spatial heterogeneity. During 2000–2018, the regions with vegetation improvement (72.87%) were much greater than that with degradation (26.55%) in the YRB (IMS). Annual precipitation change (4.55%) was a key driving factor to the vegetation coverage change in the YRB (IMS). Among the four sub-regions, the land use conversion type demonstrated the largest explanatory power, but the q values of the four sub-regions were different from each other. The results of the interaction showed that land use change and annual precipitation change were the major driving factors that influenced regional vegetation coverage change. This study has an important reference value for improving the basin's ecological environment.

Keywords Vegetation coverage · Landscape pattern · Human activities · Climate change · Geographic detectors

Introduction

Vegetation, covering about 20% of the Earth's surface, is an important component of the terrestrial ecosystem (Li et al. 2017; Daham et al. 2018). Vegetation coverage change has a great influence on natural ecosystem services and brings many impacts on human survival and life (Lawley et al. 2016). Meanwhile, vegetation dynamics are sensitive to human disturbance and climate change (Vereecken et al. 2010; Wang et al. 2015; Zhang and Huang 2019). Temperature and precipitation are major meteorological factors affecting regional vegetation conditions (Wen et al. 2017; Zhang and Huang 2019). Precipitation is an important supply source of soil moisture, which affects vegetation growth (Yuan et al. 2019). Temperature could affect plant growth by influencing photosynthesis, respiration, and transpiration (Peng et al. 2013). Human activities also greatly changed the vegetation coverage. For example, a series of ecological restoration programs, including the Three-North Shelterbelt Project (TNSP), the Nature Forest Conservation Program (NFCP), the Beijing-Tianjin Sand Source Control Program

Responsible Editor: Philippe Garrigues

✉ Chesheng Zhan
zhancs@igsnrr.ac.cn

[1] State Key Laboratory of Resources and Environmental Information Systems, Institute of Geographic Sciences and Natural Resources Research, Chinese Academy of Sciences, Beijing 100101, China

[2] Key Laboratory of Water Cycle and Related Land Surface Processes, Institute of Geographic Sciences and Natural Resources Research, Chinese Academy of Sciences, Beijing 100101, China

[3] Key Laboratory of Ecosystem Network Observation and Modeling, Institute of Geographic Sciences and Natural Resources Research, Chinese Academy of Sciences, Beijing 100101, China

[4] University of Chinese Academy of Sciences, Beijing 100049, China

(BSSCP), and the Grain for Green Project (GTGP) were implemented to improve ecological environment in China. These programs have improved vegetation coverage by protecting natural forests and planting trees protecting natural forests (Zhou et al. 2009; Wu et al. 2013; Zhang et al. 2016). Other human activities, such as the expansion of farmland, mining, urbanization, and overgrazing, could reduce the vegetation coverage in some regions (Hilker et al. 2014; Wang et al. 2015; Du et al. 2019; Yan et al. 2020).

The driving mechanism of vegetation dynamics has become a research hotspot. Some mathematical methods have been introduced, including statistical methods and models (like regression analysis and correlation analysis) (Ma et al. 2007; Wang et al. 2015; Chen et al. 2017; Feng et al. 2019; Yan et al. 2020) have been widely applied to ascertain the contributions of driving factors to vegetation variation. However, these methods are applicable when there is a linear relationship between driving factors and vegetation variation (Zhu et al. 2020). Nonlinear responses of vegetation variations to climate change such as abrupt change may also exist (Liu and Lei 2015). As a new statistical method, geographic detectors could detect spatial heterogeneity. Its q statistics could quantify the contribution of a single detection factor and interaction intensity between two detection factors (Wang and Xu 2017). In recent years, geological detectors were commonly used for attribution analysis of vegetation change. For example, Peng et al. (2019) analyze the impact of natural factors on vegetation change by geographic detectors and reveal soil types, elevation, and annual mean temperature which are the key natural factors affecting vegetation change in Sichuan province. Zhu et al. (2020) illustrate natural and anthropogenic factors on vegetation change and reveal land use conversion type could explain 23.9% and interaction between precipitation and land use conversion type could explain 36.0% of NDVI changes in the Heihe River Basin.

The relationship between driving factors and vegetation conditions is characterized by geographical heterogeneity (Qu et al. 2018). For example, rainfall has a positive function on vegetation growth in most water-deficient areas. However, heavy rainfall poses an inhibition effect on the vegetation growth in humid regions (Xu et al. 2014; Liu and Lei 2015). In the ecologically fragile area, human disturbance and climate change have been considered as major causes of land degradation (Tian et al. 2015; Shen et al. 2018; Han et al. 2021). The Yellow River Basin, with a fragile ecological environment, is an important economic zone and ecological functional zone in China (Jiang et al. 2021). In the last few decades, with the disturbance of different driving factors, the vegetation coverage has changed dramatically (Jiang et al. 2015). Some relevant conclusions have been drawn from previous research: The vegetation coverage in the west and southeast is better than that in the northwest, and the regions with improved vegetation coverage are larger than that with degraded vegetation coverage (Jiang et al. 2015; Li et al. 2019). Meanwhile, the response of vegetation growth to climate change has significant spatial differences (Miao et al. 2012; Li et al. 2019). The YRB (IMS) is an important ecological protection zone and environmental governance zone. Such as, the Hetao Irrigation district is distributed in the north of reach, which is an important agricultural area. To a certain extent, the development of irrigated agriculture could improve the regional ecological environment. The Hobq Desert, with a dry climate and severe sandstorm, is in the south of reach. The ecological environment in the YRB (IMS) is greatly different, revealing the driving mechanism of its vegetation change, which could provide a scientific basis for improving the basin ecosystem. However, previous research in this area is focused on runoff, water resource, and eco-environmental aspects (Huang et al. 2016a), and ascertaining the influence of human activities and climate factors on vegetation variation in the YRB (IMS) is still insufficient.

The normalized difference vegetation index (NDVI) could reflect the terrestrial vegetation productivity and growth status and is commonly applied in the research of vegetation coverage change and its driving mechanism (Potter and Brooks 1998; Zhao et al. 2018; Hu and Xia 2019; Yang et al. 2021). In this paper, long time series NDVI datasets were used to monitor vegetation coverage change of the YRB (IMS). Then, geographic detectors were used to reveal the effects of detection factors on vegetation variation in the YRB (IMS) and four sub-regions. The objectives are to (1) detect the vegetation coverage dynamics from 2000 to 2018 and (2) quantify the contributions of detection factors to vegetation coverage change and identify major driving factors over different sub-regions.

Materials and methods

Study area

The YRB (IMS) (39–42° N, 106–113° E) is located in southwest Inner Mongolia in China (Fig. 1), with an area of about 9.6×10^4 km^2. Annual precipitation was gradually increasing from the west to the east, ranging from 130 to 450 mm. Annual mean temperature was gradually increasing from the northeast to the southwest, ranging from 5 to 9 ℃. Grassland and cropland are the primary land cover types. Major topography types include Hetao Plain, Yin Mountains, and Ordos Plateau.

The YRB (IMS) is divided into four sub-regions based on the typical water system: the Hetao Irrigation district (HTID), located in Hetao Plain, with flat terrain, fertile soil, and irrigation diverting from the Yellow River, is an important grain yielding area; the Ten Tributaries region (TTR)

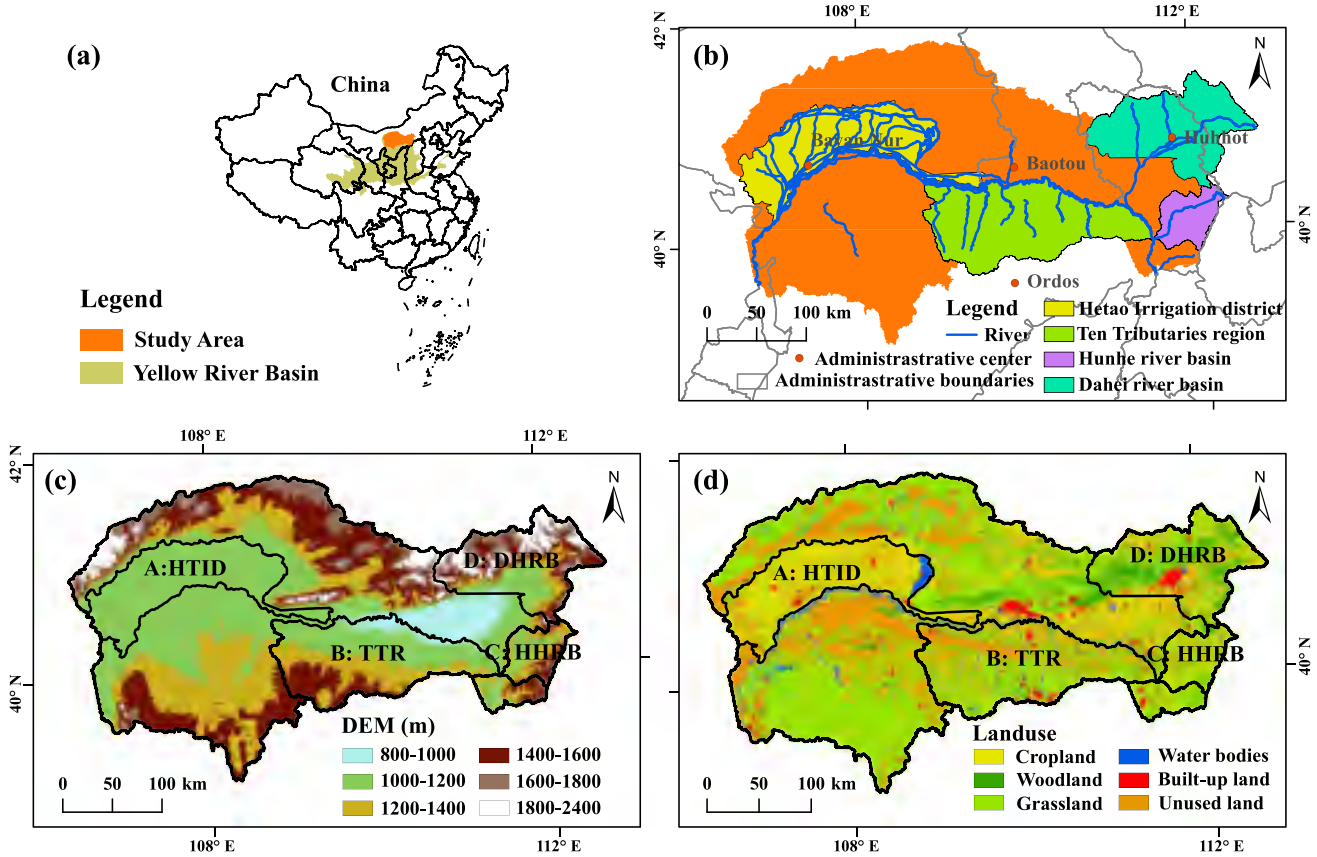

Fig. 1 The location (**a**), sub-regions (**b**), elevation (**c**), and land use types (**d**) of the study area (*HTID*, Hetao Irrigation district; *TTR*, Ten Tributaries region; *HHRB*, Hunhe river basin; *DHRB*, Dahei river basin)

is the main sediment yielding area in the YRB (IMS) as a result of abominable natural conditions and serious soil erosion; the Hunhe river basin (HHRB), located in Hilly and Gully Area with Loess, suffer frequent drought and serious soil erosion; the Dahei river basin (DHRB) consists of plains and mountains regions, which is affected by drought, flood hazards, and salt-alkaline. The water system of DHRB has a fixed flow path in mountains and is intertwined with irrigation channels in the plains owing to serious human disturbances. Therefore, we excluded the mountains area in our research.

Data

The 16-day MODIS NDVI datasets (250 m × 250 m) were downloaded from the MOD13Q1 series products (http://modis.gsfc.nasa.gov). Pre-processing steps include format converting, reprojecting, and extracting. To minimize the influence of clouds, solar elevation angle, and atmosphere, the maximum value compositing (MVC) method (Holben 1986; Stow et al. 2007) was applied to obtain yearly NDVI data.

The monthly meteorological data from 2000 to 2018 at twenty-four meteorological stations in and around the YRB (IMS), including precipitation, temperature, relative humidity, and sunshine duration, were provided by the China Meteorological Data Service Center (http://data.cma.cn). Finally, monthly data was processed into yearly data, the annual precipitation (annual sunshine duration) was the sum of the monthly precipitation (monthly sunshine duration) from January to December, and the annual mean temperature (annual mean relative humidity) was calculated as the mean temperature (relative humidity) from January to December. In this paper, we used the Kriging interpolation method to obtain the spatial distribution of meteorological data with the same resolution of NDVI (Liu et al. 2019).

The land use cover data (30 m × 30 m) in 2000 and 2018 were available from the Data Center for Resources and Environmental Sciences, Chinese Academy of Sciences (RESDC) (http://www.resdc.cn). The land use types were classified into 6 first-grade types (cropland, woodland, grassland, water bodies, built-up land, and unused land) according to the China land use/cover remote sensing classification system. And we used the digital elevation model (DEM) data with a 30 m spatial resolution was derived from the

Geospatial Data Cloud (http://www.gscloud.cn). The data of the effective irrigation, the total sown of crops, and the afforestation area was from the Statistical Yearbook of Inner Mongolia.

Methods

Vegetation coverage calculation

Vegetation coverage could be inversed by the dimidiate pixel model, which is commonly used in dynamic monitoring of vegetation (Gutman and Ignatov 1998; Hao et al. 2020):

$$VC = \frac{NDVI - NDVI_{soil}}{NDVI_{veg} - NDVI_{soil}} \times 100\% \quad (1)$$

where, *VC* represents vegetation coverage, $NDVI_{soil}$ represents the *NDVI* value of vegetation free area or bare soil, and $NDVI_{veg}$ represents the *NDVI* value of the area covered completely by vegetation. To minimize the influence of the atmosphere and different surface conditions, considering the real situation of vegetation in the YRB (IMS) and the *NDVI* cumulative frequencies table, we extracted a cumulative probability of about 0.5% and 99.5% to represent $NDVI_{soil}$ and the $NDVI_{veg}$, respectively. *VC* is divided into five levels: $VC \le 10\%$ (bare soil), $10\% < VC \le 30\%$ (low), $30\% < VC \le 45\%$ (medium–low), $45\% < VC \le 60\%$ (medium), $VC > 60\%$ (high).

Landscape pattern indices

Landscape index, a quantitative index, can express and reflect the information the structure and spatial form of landscape pattern (Hao et al. 2017; Zhang et al. 2020b). In this paper, we used four landscape pattern indices to reveal the changes of vegetation landscape fragmentation and agglomeration in the landscape level: (1) number of patches (NP) reflecting the degree of fragmentation of the landscape, (2) landscape division index (DIVISION) indicating the degree of patch dispersion of the same landscape type, (3) contagion index (CONTAG) describing the degree of agglomeration and elongation of different patch types (units:%), and (4) Shannon's diversity index (SHDI) representing the proportion abundance of each patch type and the heterogeneity of the landscape. The four indexes could be calculated by Fragstats 4.2 software.

Trend analysis

Sen's slope (Sen 1968), which could effectively decrease the influence of outliers, was used to estimate the slope of the trend. Mann–Kendall (Mann 1945; Kendal 1975) statistical test is a nonparametric test method, which could objectively reveal the time series change trend. The Sen + Mann–Kendall was widely being used to analyze long-term sequences of vegetation coverage change (Feng et al. 2019; Zhang et al. 2020a).

$$slope = \text{Median}\left(\frac{x_j - x_i}{j - i}\right)(1 < i < j < n) \quad (2)$$

$$S = \sum_{i=1}^{n-1} \sum_{j=j+1}^{n} \text{sgn}\left(x_j - x_i\right) \quad (3)$$

$$\text{sgn}\left(x_j - x_i\right) = \begin{cases} +1, x_j - x_i > 0 \\ 0, x_j - x_i = 0 \\ -1, x_j - x_i < 0 \end{cases} \quad (4)$$

$$\text{Var}(S) = \frac{n(n-1)(2n+5) - \sum_{i=1}^{m} t_i(t_i - 1) - (2t_i + 5)}{18} \quad (5)$$

$$Z = \begin{cases} \frac{S-1}{\sqrt{\text{VAR}(S)}}, S > 0 \\ 0, S = 0 \\ \frac{s+1}{\sqrt{\text{VAR}(S)}}, S < 0 \end{cases} \quad (6)$$

where, slope is the vegetation change trend, a slope > 0 represents vegetation improvement, and a slope < 0 represents vegetation degradation. *n* represents the length of the dataset. x_i and x_j represent the *VC* values of the pixel in the year *i* and *j*, respectively. Additionally, t_i represents the width of the knot (number of data with identical *VC* values in group i). We used a two-sided test and given significance level $a = 0.05$, if $|Z| > 1.96$, then reject the original hypothesis, the time series shows a significant change.

Geographic detectors

In this study, geographic detectors were applied to ascertain the contributions of detection factors to spatial heterogeneity to vegetation coverage change in the YRB (IMS) and four sub-regions (the HTID, the TTR, the HHRB, and the DHRB). The vegetation coverage change trend from 2000 to 2018 was regarded as the dependent variable *Y*. Potential driving factors, including land use conversion type from 2000 to 2018, annual precipitation change trend, annual mean relative humidity change trend, annual mean temperature change trend, and annual sunshine duration change trend from 2000 to 2018, were selected as the detection factors *X*. The discrete variables were required as input data of geographic detectors, thus, the direct bisection method was used to discretize the independent variables (Table 1). The spatial distribution of detection factors *X* and vegetation coverage change trend *Y* is shown in Fig. 2.

Table 1 Discretization of continuous numerical independent variables

Discretization	Detection factors			
	X1 Annual precipitation change trend (mm year^{-1})	X2 Annual mean temperature change trend (℃ year^{-1})	X3 Annual mean relative humidity change trend (year^{-1})	X4 Annual sunshine duration change trend (h year^{-1})
1	− 2–0	− 0.066 to − 0.044	− 0.4 to − 0.3	− 14.8 to − 7.4
2	0–2	− 0.044 to − 0.022	− 0.3 to − 0.2	− 7.4–0.0
3	2–4	− 0.022–0.000	− 0.2 to − 0.1	0.0–7.4
4	4–6	0.000–0.022	− 0.1–0.0	7.4–14.8
5	6–8	0.022–0.044	0.0–0.1	14.8–22.2
6	8–10	0.044–0.066	0.1–0.2	22.2–29.6

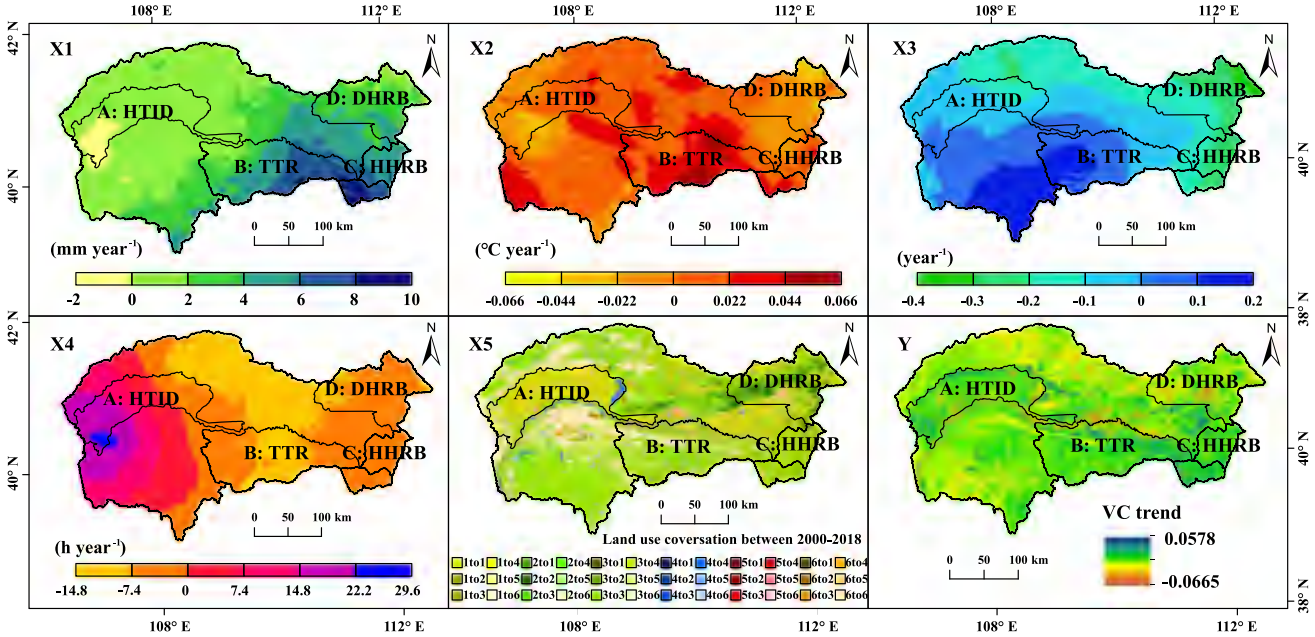

Fig. 2 The spatial distribution of (X_1) annual precipitation change trend, (X_2) annual mean temperature change trend, (X_3) annual mean relative humidity change trend, (X_4) annual sunshine duration change trend, (X_5) land use conversion type and (Y) vegetation coverage change trend (1, cropland; 2, woodland; 3, grassland; 4, water bodies; 5, built-up land; 6, unused land; *HTID*, Hetao Irrigation district; *TTR* , Ten Tributaries region; *HHRB*, Hunhe river basin; *DHRB*, Dahei river basin)

Geographic detectors include four sub-detectors:

(1) Factor detector:

Factor detector could ascertain the influence of detection factors on the spatial heterogeneity of vegetation variation. The contribution of X to the spatial heterogeneity of Y could be expressed as $q \times 100\%$, and the stronger the influence of detection factors of vegetation coverage change. q value could be simply transformed to satisfy the non-central F distribution and determine the level of significance (Wang et al. 2016):

$$q = 1 - \frac{\sum_{h=1}^{L} N_h \sigma_h^2}{N\sigma^2} \tag{7}$$

where, h is the stratification of the vegetation change or the detection factors; N_h and N represent the units in class h and the whole region, respectively; ${\sigma_h}^2$ and σ^2 represent the variance of Y value in class h and the whole region, respectively.

(2) Interaction detector:

Interaction detector is appropriate to detect the effect of the joint action of detection factors X_a and X_b on the spatial

heterogeneity of vegetation variation. Five results of interaction are as follows:

1) non-linear weakness: $q(X_a \cap X_b) < \min[q(X_a), q(X_b)]$;
2) single-factor non-linear weakness: $\min[q(X_a), q(X_b)] < q(X_a \cap X_b) < \max[q(X_a), q(X_b)]$;
3) independent: $q(X_a \cap X_b) = q(X_a) + q(X_b)$;
4) two-factor enhancement: $q(X_a \cap X_b) > \max[q(X_a), q(X_b)]$;
5) non-linear enhancement: $q(X_a \cap X_b) > q(X_a) + q(X_b)$.

(3) Ecological detector:

Ecological detector could use F statistics to measure the influence of two detection factors on the spatial pattern of vegetation coverage change is significant difference (*Y*) or no significant difference (*N*):

$$F = \frac{N_{X1}(N_{X2} - 1)SSW_{X1}}{N_{X2}(N_{X1} - 1)SSW_{X2}} \tag{8}$$

$$SSW_{X1} = \sum_{h=1}^{L1} N_h \sigma_h^2 \tag{9}$$

$$SSW_{X2} = \sum_{h=1}^{L2} N_h \sigma_h^2 \tag{10}$$

where, N_{X1} and N_{X2} are the number of samples for detection factors X_1 and X_2, respectively. L_1 and L_2 are the numbers of stratifications for detection factors X_1 and X_2, respectively. SSW_{X1} and SSW_{X2} represent the total intra-layer variances of the stratification formed by X_1 and X_2, respectively.

(4) Risk detector:

Risk detector could use t statistic to test whether there is a significant difference in the attribute average value between two sub-regions. It could be used to judge the suitable range/type of each detection factor:

$$t_{\bar{y}_{h=1} - \bar{y}_{h=2}} = \frac{\overline{Y}_{h=1} - \overline{Y}_{h=2}}{\left[\frac{Var\left(\overline{Y}_{h=1}\right)}{n_{h=1}} + \frac{Var\left(\overline{Y}_{h=2}\right)}{n_{h=2}}\right]^{\frac{1}{2}}} \tag{11}$$

where, n_h represents the number of samples of the detection factor at layer h; $\overline{Y}_h$ represents the mean value of vegetation coverage change trend of the detection factor at layer h; Var is variance.

Results

Landscape pattern analysis

In terms of the landscape level, NP decreased from 2000 to 2011 with a slope of − 616.4300 and increased from 2011 to 2018 with a slope of 1068.2000. The minimum NP was found in 2011 (42,340), showing that the fragmentation degree of vegetation landscape gradually decreased before 2011, and the small patches gradually shifted to large patches. In contrast, the fragmentation degree of vegetation landscape gradually increased since 2011, with small patches gradually increasing and the degree of spatial heterogeneity increasing (Fig. 3a); DIVISION increased from 2000 to 2009 (0.0016) and decreased from 2009 to 2018 (− 0.0015). During the past 19 years, the maximum value was found in 2009 (0.96), showing that the separation degree of vegetation landscape in the YRB (IMS) gradually increased from 2000 to 2009. In contrast, the separation degree of vegetation landscape gradually decreased from 2009 to 2018. The overall landscape type was composed of multiple small patches, with a relatively high degree of fragmentation (Fig. 3b); CONTAG increased from 2000 to 2018 with a slope of 0.0675, indicating that patches connectivity features an increasing trend (Fig. 3c); SHDI decreased from 2000 to 2018 with a slope of − 0.0011, indicating that vegetation landscape diversity characterizes a decreasing trend (Fig. 3d). The result suggested that the vegetation landscape was composed of small patches with a high degree of fragmentation, but the patch connectivity has increased in recent years.

Temporal-spatial variation of vegetation coverage, climate, and LUCC

As shown in Fig. 4 from 2000 to 2018, the vegetation coverage in the YRB (IMS) ranged from 0.32 to 0.46, with the minimum and maximum vegetation coverage occurring in 2001 (0.32) and 2018 (0.46), respectively. The vegetation coverage showed a slight fluctuating upward trend at an averaged increasing rate of 0.0034 year^{-1}. The HTID showed the highest vegetation coverage, followed by the DHRB, HHRB, and TTR. The DHRB and HHRB showed similar temporal variation trends.

Over the past 19 years, vegetation coverage change in the YRB (IMS) showed remarkable spatial heterogeneity (Figs. 2Y and 5). The vegetation coverage in most areas (72.87%) showed an increasing trend, in which 27.19% area pass the 95% significant level. Especially in the HTID, TTR, and HHRB, the vegetation coverage has been significantly improved. The area with decreasing trend occupied over 26.55% of the study area, the significant degradation areas (3.32%) mainly distributed in the built-up land and along the Yellow River. Among the four sub-regions, the area with the vegetation improvement was far greater than the degradation. The most obvious decrease area was found in the DHRB, with the decreasing area occupying over 39.20%.

From 2000 to 2018, the annual precipitation and annual mean temperature exhibited a slight fluctuating upward

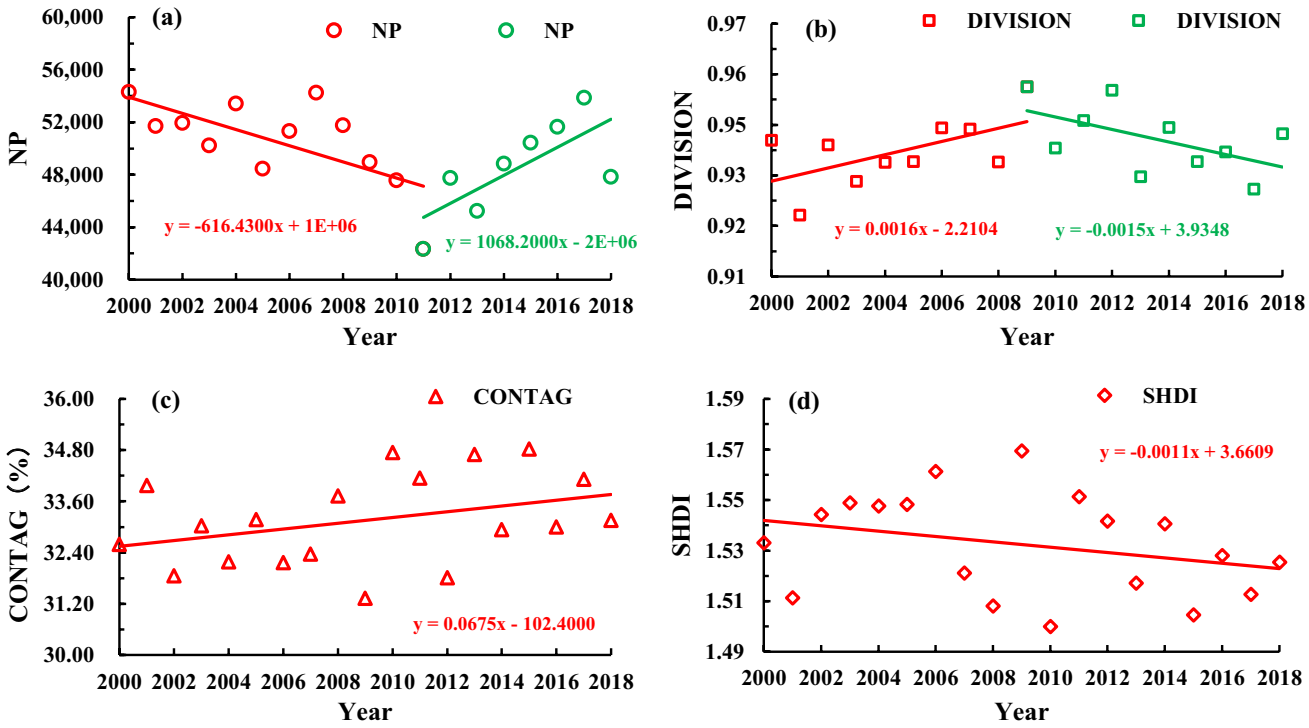

Fig. 3 Landscape pattern indexes from 2000 to 2018 under the landscape level

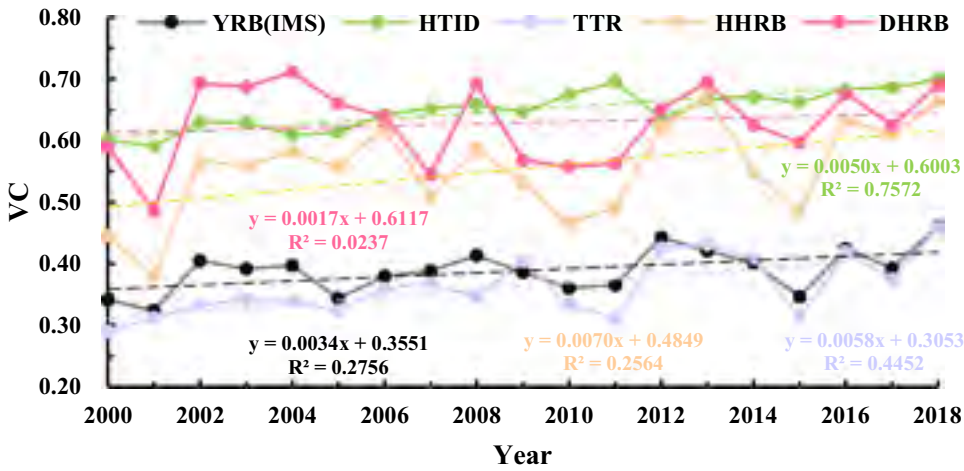

Fig. 4 The interannual variation of vegetation coverage from 2000 to 2018 (*HTID*, Hetao Irrigation district; *TTR*, Ten Tributaries region; *HHRB*, Hunhe river basin; *DHRB*, Dahei river basin)

trend with an average increasing rate of 2.5894 mm year^{-1} and 0.0100 ℃ year^{-1}, respectively (Fig. 6a and b). Mean annual temperature in the DHRB showed a slight fluctuating downward trend (− 0.0120 ℃ year^{-1}). Spatially, the area with precipitation increased occupying approximately 96.78% of our study area. Decreasing precipitation mostly happened in the western part of the YRB (IMS) (Fig. 2 (X1)); Areas with temperature increasing accounting for approximately 75.64% of the study area (Fig. 2 (X2)). The result suggested that the weather condition in the YRB (IMS) were getting warmer and wetter. Annual mean relative humidity and annual sunshine duration showed a slight fluctuating downward trend with an average decreasing rate of − 0.0970 year^{-1} and − 1.7075 h year^{-1}, respectively (Fig. 6c and d). Annual sunshine duration in the HTID exhibited a slight fluctuating upward trend (6.0833 h year^{-1}). The change trend of relative humidity was gradually increasing from northeast to southwest (Fig. 2 (X3)). About 66.88% of the area in the YRB (IMS) showed a decreasing trend in sunshine duration, whereas the increasing trend mainly happened in the western YRB (IMS) (Fig. 2 (X4)).

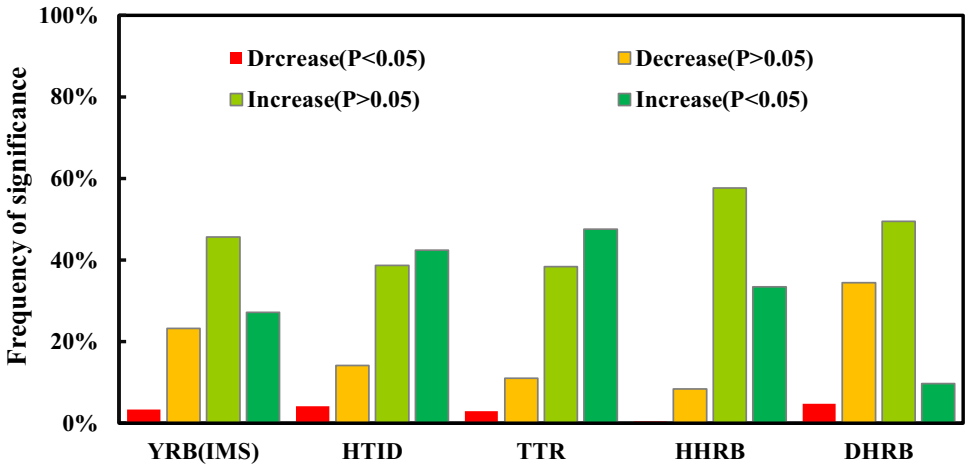

Fig. 5 Frequencies of the significance of vegetation coverage change trends from 2000 to 2018 (*HTID*, Hetao Irrigation district; *TTR*, Ten Tributaries region; *HHRB*, Hunhe river basin; *DHRB*, Dahei river basin)

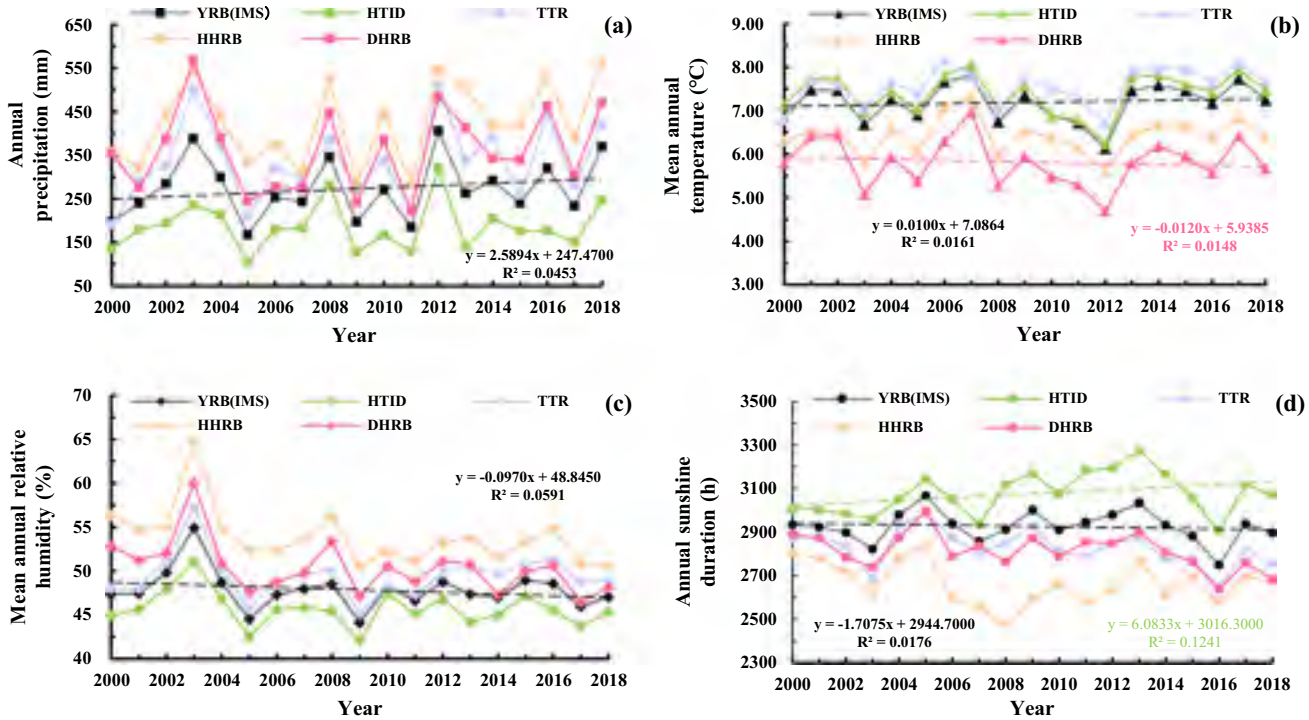

Fig. 6 Temporal variations of **a** annual precipitation, **b** mean annual temperature, **c** mean annual relative humidity, and **d** annual sunshine duration during 2000–2018 (*HTID*, Hetao Irrigation district; *TTR*, Ten Tributaries region; *HHRB*, Hunhe river basin; *DHRB*, Dahei river basin)

During the past 19 years, there were approximately 7610.66 km^2 of land whose land types have changed. The noticeable change is that the overall grassland area decreased by 1573.48 km^2 and the built-up land area increased by 1383.28 km^2 (Fig. 7a). The increase in built-up land benefited from the conversion of grassland (787.97 km^2) and cropland (521.93 km^2). The decrease in grassland was attributed to the transfer into cropland (1286.45 km^2), built-up land (787.97 km^2), and unused land (711.61 km^2) (Fig. 2 (X5)). The area of cropland only increased by 105.47 km^2, but the conversion between cropland and grassland was intense. Cropland was mainly transferred into grassland (682.21 km^2) and built-up land (521.93 km^2). At the same time, grassland (1286.45 km^2) was transferred into cropland, which compensated for the loss of cropland.

Among the four sub-regions (Figs. 7b and 2 (X5)), the noticeable change is that the built-up land area increased by 326.79 km^2 in the TTR, which was mainly converted from grassland (212.85 km^2). Grassland area decreased by 333.16 km^2, which was mainly transferred into built-up land (212.85 km^2), cropland (197.35 km^2), and unused land (111.49 km^2). In the HHRB, cropland was mainly transferred into

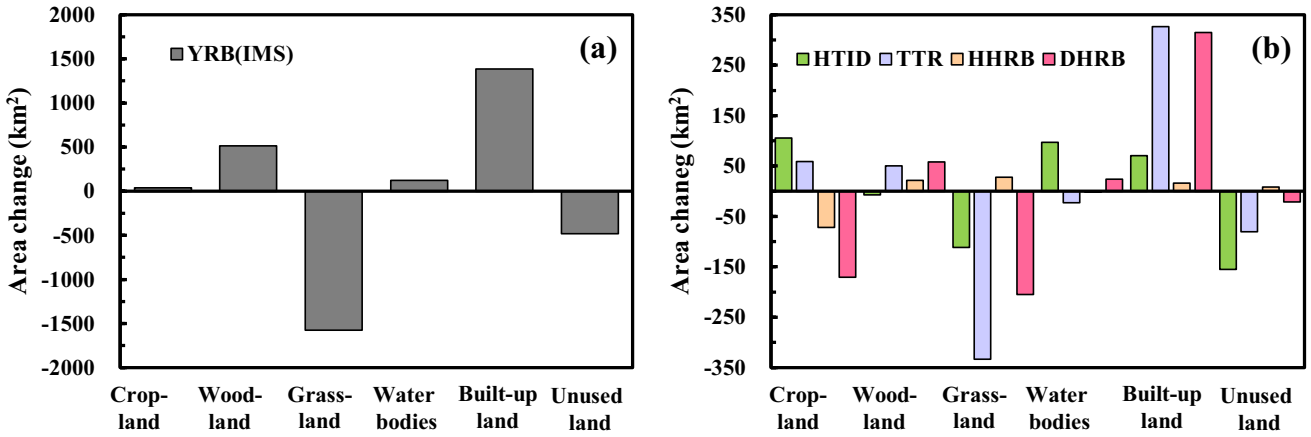

Fig. 7 Change of land use types from 2000 to 2018 (*HTID*, Hetao Irrigation district; *TTR*, Ten Tributaries region; *HHRB*, Hunhe river basin; *DHRB*, Dahei river basin)

Table 2 The *q* value of each detection factor derived from geographic detectors

Detection factors	HTID	TTR	HHRB	DHRB	YRB (IMS)
X_1	0.0071	0.0430	0.0054	0.0153	0.0455
X_2	0.0280	0.0014	0.0188	0.0073	0.0024
X_3	0.0203	0.0526	0.0063	0.0293	0.0060
X_4	0.0340	0.0146	0.0184	0.0230	0.0171
X_5	0.0701	0.0808	0.0492	0.1012	0.0401

Note: X_1, annual precipitation change trend; X_2, annual mean temperature change trend; X_3, annual mean relative humidity change trend; X_4, annual sunshine duration change trend; X_5, land use conversion type; *HTID*, Hetao Irrigation district; *TTR*, Ten Tributaries region; *HHRB*, Hunhe river basin; *DHRB*, Dahei river basin

grassland (101.37 km^2), which resulted in a decrease in cropland (71.86 km^2). In the HTID, the increase in cropland benefited from the conversion of grassland (235.68 km^2). In the DHRB, built-up lands area increased by 314.89 km^2, which was mainly converted from cropland (162.45 km^2) and grassland (139.71 km^2).

Attribution of vegetation coverage change

Impact of different detection factors of vegetation variation

As shown in Table 2, the annual precipitation change trend showed the largest explanatory power of 4.55% in the YRB (IMS). In addition, the corresponding explanatory power of other detection factors from high to low were land use conversion type (4.01%) > annual sunshine duration change trend (1.71%) > annual mean relative humidity change trend (0.60%) > annual mean temperature change trend (0.24%). In the four sub-regions, the land use conversion type demonstrated the largest explanatory power, but the *q* values of the four sub-regions were different from each other. Among the four sub-regions, land use conversion type showed the most significant influence in DHRB (10.12%), followed by that in the TTR (8.08%), HTID (7.01%), and HHRB (4.92%). This result implied that the impact of land use change on vegetation coverage in the DHRB was greater than that in the TTR, HTID, and HHRB.

Significant differences between driving factors

As shown in Fig. 8, in the YRB (IMS), there is a significant impact between annual precipitation change trend (land use conversion type) and other detection factors except for land use conversion type (annual precipitation change trend) on the spatial heterogeneity of vegetation coverage change. The result suggested that annual precipitation change and land use change have a greater effect on vegetation change. Among the four sub-regions, we found that there was a significant difference between land use conversion and other detection factors of vegetation variation. The result verified that land use conversion type was a key driving factor that influenced vegetation change in the sub-regions.

Interaction between driving factors

In the YRB (IMS), the spatial heterogeneity of vegetation change was the result of the joint action of various driving factors, and most types of driving factor interactions were non-linear enhancement except for the bilinear mutual enhancement between annual precipitation change trend and annual sunshine duration change trend. As shown in Fig. 9, the interaction between annual precipitation change trend and land use conversion type revealed the largest

YRB(IMS)	X1	X2	X3	X4	X5
X1					
X2	Y				
X3	Y	N			
X4	Y	N	N		
X5	N	Y	Y	Y	

HTID	X1	X2	X3	X4	X5
X1					
X2	N				
X3	N	N			
X4	Y	N	N		
X5	Y	Y	Y	Y	

TTR	X1	X2	X3	X4	X5
X1					
X2	Y				
X3	N	Y			
X4	Y	N	Y		
X5	Y	Y	Y	Y	

HHRB	X1	X2	X3	X4	X5
X1					
X2	N				
X3	N	N			
X4	N	N	N		
X5	Y	Y	Y	Y	

DHRB	X1	X2	X3	X4	X5
X1					
X2	N				
X3	N	Y			
X4	N	N	N		
X5	Y	Y	Y	Y	

Fig. 8 Statistical significance of detection factors (note: 95% confidence level. "Y" denotes a significant difference and "N" denotes a no significant difference) (X_1, annual precipitation change trend; X_2, annual mean temperature change trend; X_3, annual mean relative humidity change trend; X_4, annual sunshine duration change trend; X_5, land use conversion type)

YRB(IMS)	X1	X2	X3	X4	X5
X1	0.0455				
X2	0.0521	0.0024			
X3	0.0579	0.0200	0.0060		
X4	0.0625	0.0321	0.0421	0.0171	
X5	0.1315	0.0728	0.0754	0.0897	0.0401

HTID	X1	X2	X3	X4	X5
X1	0.0071				
X2	0.0532	0.0280			
X3	0.0254	0.0598	0.0203		
X4	0.0469	0.0699	0.0583	0.0341	
X5	0.1101	0.1204	0.1184	0.1369	0.0701

TTR	X1	X2	X3	X4	X5
X1	0.0430				
X2	0.0669	0.0014			
X3	0.0707	0.0720	0.0526		
X4	0.0675	0.0279	0.0658	0.0146	
X5	0.1565	0.1005	0.1618	0.1141	0.0808

HHRB	X1	X2	X3	X4	X5
X1	0.0054				
X2	0.0473	0.0188			
X3	0.0428	0.0567	0.0063		
X4	0.0423	0.0472	0.0345	0.0184	
X5	0.0782	0.0865	0.0722	0.0857	0.0492

DHRB	X1	X2	X3	X4	X5
X1	0.0153				
X2	0.0376	0.0073			
X3	0.0424	0.0635	0.0293		
X4	0.0577	0.0483	0.0728	0.0230	
X5	0.1319	0.1442	0.1551	0.1533	0.1012

Fig. 9 Influence of the interactions among different detection factors to vegetation variation (X_1, annual precipitation change trend; X_2, annual mean temperature change trend; X_3, annual mean relative humidity change trend; X_4, annual sunshine duration change trend; X_5, land use conversion type)

explanatory power of 13.15% in the YRB (IMS). The result suggested that the coupling between annual precipitation change trend and land use conversion type was the main driving factor to vegetation coverage change trend.

Adaptation range or type suitable of driving factors to vegetation coverage change

The risk detector results could reflect the differences in the vegetation coverage change of each sub-region (Fig. 10, Table 3). In the YRB (IMS), the vegetation coverage change trend increased with the increasing annual precipitation change trend, indicating that rainfall has an active effect on vegetation growth. The vegetation coverage change trend reached the maximum in the annual precipitation change trend range 8–10 mm year^{-1}. Compared to annual precipitation change, other climate factors had less impact on vegetation coverage change. The result further proved that precipitation was a key driving factor of vegetation growth.

In the HTID, when annual precipitation change trend in the range of − 1.2 to − 0.6 mm year^{-1}, the vegetation coverage change trend reached the maximum, indicating that vegetation growth was better when precipitation reduces to a certain extent. In the TTR, the vegetation coverage change trend increased with the increasing annual precipitation change trend, indicating the increase of precipitation was more suitable for vegetation growth. In the HHRB, the vegetation coverage change trend decreased with the increasing annual sunshine duration change trend, even in the range − 3.2 to − 2.4 h year^{-1}, which could cause the inhibition of vegetation growth. In the DHRB, the vegetation coverage change trend increased with the increasing annual sunshine duration change trend. Annual sunshine duration change trend and annual mean relative humidity change

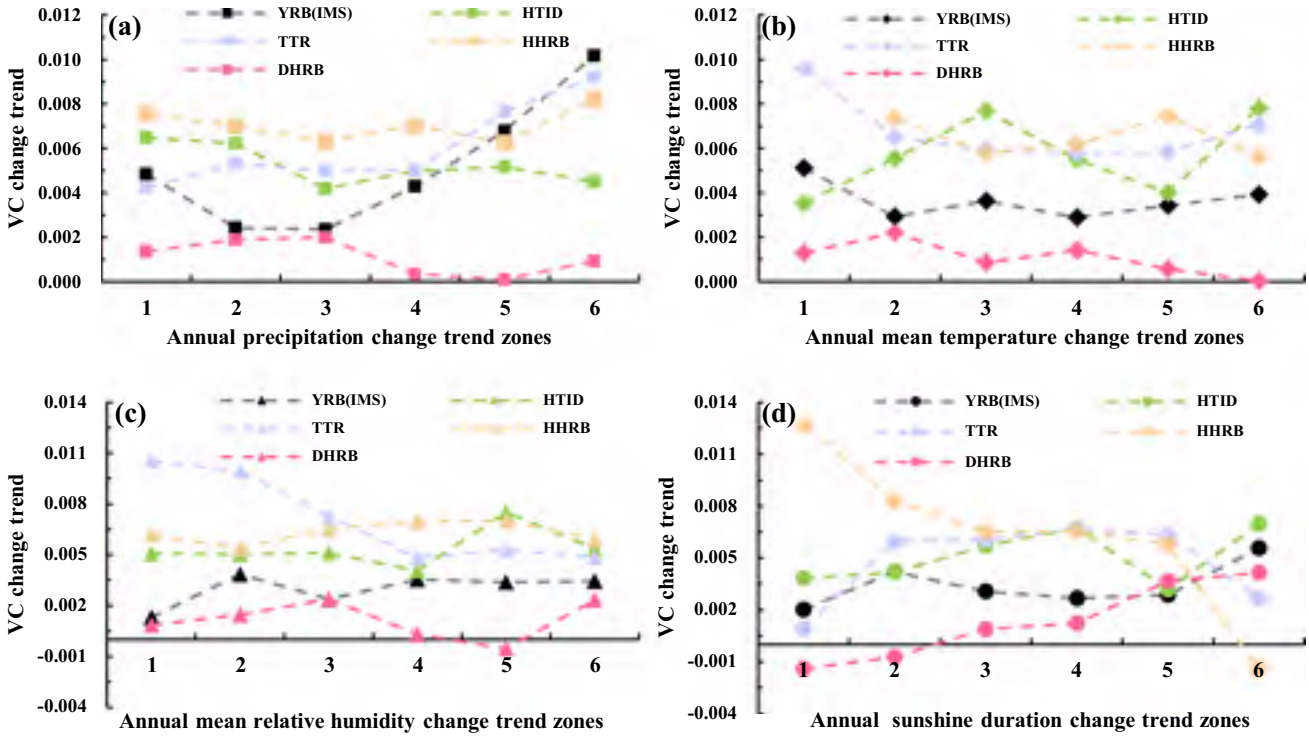

Fig. 10 Vegetation coverage change trend in different zones of **a** annual precipitation change trend, **b** annual mean temperature change trend, **c** annual mean relative humidity change trend, and **d** andannual mean sunshine duration change trend (*HTID*, Hetao Irrigation district; *TTR*, Ten Tributaries region; *HHRB*, Hunhe river basin; *DHRB*, Dahei river basin)

Table 3 The suitable range/type of detection factors

Regions	X1	X2	X3	X4
YRB (IMS)	8–10	− 0.066 to − 0.044	− 0.3 to − 0.2	22.2–29.6
HTID	− 1.2 to − 0.6	0.024–0.036	0–0.06	18–24
TTR	7.5–9	− 0.0155–0	− 0.18 to − 0.12	− 6 to − 4.5
HHRB	7.2–8	0.011–0.022	− 0.21 to − 0.175	− 7.2 to − 6.4
DHRB	2.1–2.8	− 0.03 to − 0.02	− 0.25 to − 0.2	− 4.4 to − 3.3

Note: X_1, annual precipitation change trend; X_2, annual mean temperature change trend; X_3, annual mean relative humidity change trend; X_4, annual sunshine duration change trend; *HTID*, Hetao Irrigation district; *TTR*, Ten Tributaries region; *HHRB*, Hunhe river basin; *DHRB*, Dahei river basin

trend had a restrictive influence on vegetation coverage change trend in the range − 9.9 to − 7.7 h year^{-1} and − 0.15 to − 0.10 year^{-1}, respectively, meaning this range was not conducive to vegetation growth.

Based on previous research (Zhu et al. 2020) and considering the actual situation of the YRB (IMS), we did not consider the land use conversion types whose area proportion is less than 0.02%. In the YRB (IMS), there were 6 land use conversion types that showed a negative impact on vegetation coverage change, including cropland transferred into built-up land and water bodies, woodland transferred into unused land, water bodies transferred into built-up land, grassland transferred into built-up land, and unused land transferred into water bodies, indicating that these types were adverse to vegetation growth (Fig. 11). In the HTID and DHRB, when cropland was transferred into built-up land, there was a relatively high vegetation degradation rate. In the TTR, unused land was transferred into grassland with a relatively high vegetation improvement rate. In the HHRB, nearly all land use conversion types showed a positive influence on vegetation coverage change.

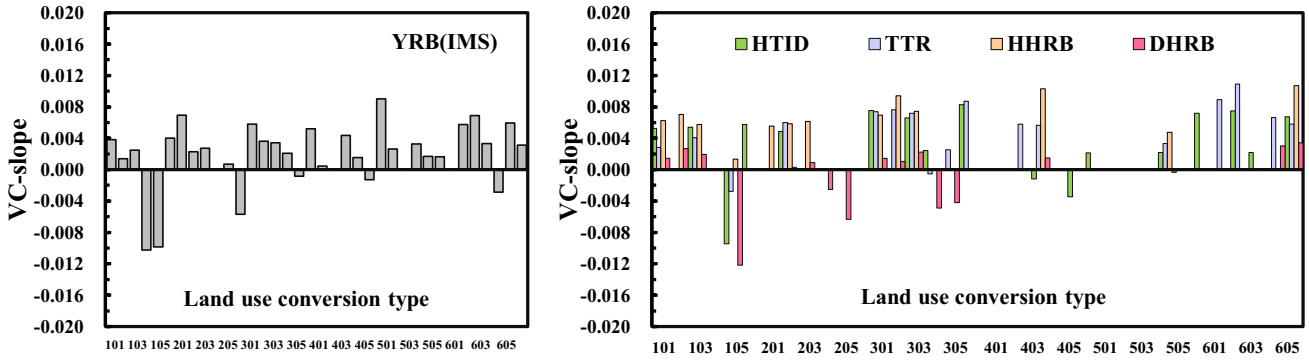

Fig. 11 Influence of land use change on vegetation variation (*HTID*, Hetao Irrigation district; *TTR*, Ten Tributaries region; *HHRB*, Hunhe river basin; *DHRB*, Dahei river basin)

Discussion

Impact of climate change on vegetation coverage change

The ecological environment was greatly improved in the Yellow River Basin, which is confirmed in previous studies (Jiang et al. 2015; Zhang et al. 2020a; Tian et al. 2021). Meteorological factors, especially the annual precipitation change trend (4.55%), had the largest explanatory power to vegetation coverage change trend. According to previous studies, precipitation was a key climate factor to promote vegetation coverage in arid and semi-arid regions (Huang et al. 2016b; Xie et al. 2016; Hua et al. 2017). However, the effects of climate change on vegetation coverage change were spatially heterogeneous. Zhang et al. (2020a) suggested that the amount of precipitation in the flood season has the most significant impact on surface vegetation of grassland and had relatively less impact on surface vegetation cover of woodland and irrigated farming areas. In the YRB (IMS), grassland was the main land use type, occupying about 46.98% of the study area (Fig. 12). In particular, most of these areas are located in regions with inadequate water resources. Thus, precipitation was a primary driving factor that controls vegetation change (Hua et al. 2017).

Among the four sub-regions, the geographical location and main surface cover types were different, thus the main climate driving factor was different. In the HTID, the effect of the precipitation change (0.71%) on vegetation coverage change was lower than that of the other detection factors. The vegetation coverage change trend decreased with the increasing annual precipitation change trend, which could be attributed to the development of irrigation agriculture. Cropland (63.37%) was the main land use type in the HTID. The main crop types were corn, wheat, and sunflower, and agricultural cultivation mainly dependent on irrigation (the average annual water diversion from the Yellow River reached 4.49×10^8 m^3) (Wang et al. 2021; Gao et al. 2021). However, in the TTR, annual mean temperature change trend (0.14%) showed the least explanatory power. Because the area of grassland occupying over 51.67% of the total area in TTR, the vegetation coverage change trend increased with

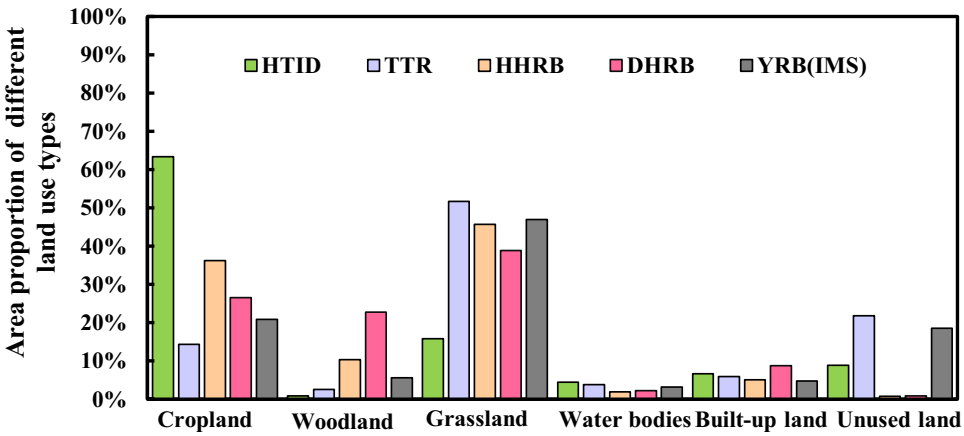

Fig. 12 Area proportion of different land use types in 2018 (*HTID*, Hetao Irrigation district; *TTR*, Ten Tributaries region; *HHRB*, Hunhe river basin; *DHRB*, Dahei river basin)

the increasing annual precipitation change trend, indicating that the growth of vegetation in this area was more dependent on precipitation than temperature. The main vegetation types include desert, sandy land, desert steppe, and typical grassland, and rainfall was the basic condition for vegetation growth (Sun et al. 2001, Li and Yang 2004; Chuai et al. 2013). Moreover, with evaporation in this region being about five to ten times precipitation, the weather condition was relatively dry (Bai et al. 2019). The increase in temperature will exacerbate the leaf transpiration of vegetation and limit the photosynthesis and growth of vegetation (Li et al. 2019; Ma et al. 2019; Zhang et al. 2020a). In the HHBR, annual mean temperature change trend (1.88%) and annual precipitation change trend (0.54%) showed the largest and least explanatory power, respectively. The result could be attributed to the relatively abundant precipitation and sufficient water resources in the HHRB. Therefore, under the condition of sufficient rainfall, increasing temperature could enhance photosynthesis, respiration, and transpiration in plants.

Impact of human activities on vegetation coverage change

Apart from meteorological factors, human activities were also a key driving factor affecting vegetation coverage. Human activities indicated by land use change, including expansion of farmland, urbanization, and afforestation, could effectively explain vegetation change (Zhu et al. 2020). Based on the geographical detectors, we found land use conversion that occurred between 2000 and 2018 was the strongest driving factor to explain the change of vegetation coverage in the four sub-regions, but the q values were different from each other. The q values of land use conversion to vegetation coverage change in the DHRB (10.12%), TTR (8.08%), and HTID (7.01%) were greater than that in the HHRB (4.92%). The result revealed that vegetation coverage in these areas was greatly affected by land use change. The growth of the population, the urban land expansion, and the rapid urbanization development resulted in gradually greater ecological and environmental problems (Ma et al. 2019; Yan et al. 2020). The original land types were disturbed by human activities, which made the vegetation coverage degenerate (Mu et al. 2013). Among the four sub-regions, the vegetation degradation that happened in the DHRB was the most noticeable. Cropland, woodland, and grassland were transferred into built-up land with a relatively high vegetation degradation rate, suggesting the built-up land in the DHRB has been greatly expanded. During the past 19 years, approximately 10% of land in DHRB and its land type has changed. The area of built-up land increased by 3.12%. The research results are in agreement with the study of Wu et al. (2018) that most of the newly added built-up land area was converted from grassland and cropland. At the same time, a lot of grasslands have been transferred into cropland to offset the loss of cropland transferred into built-up land. In the long run, urban expansion and the land use conversion type caused by the urban expansion will cause interference and damage to the regional ecological environment.

In addition, human activities have made contributions to ecosystem improvement, which has been confirmed by previous research (You et al. 2019; Chen et al. 2020; Tian et al., 2021). In the TTR, unused land was transferred into woodland and grassland with a relatively high vegetation improvement rate. Over the past 18 years, ordos had the largest cumulative afforestation area (Fig. 13). In particular, the vegetation coverage has been significantly improved in the Hobq Desert. Tian et al. (2015) showed that vegetation restoration was mainly caused by ecological restoration programs in the Hobq Desert, such as "Artificial Forestation" and "Closing Hillsides to Facilitate Afforestation," as well as the forestry ecological engineering construction such as "the

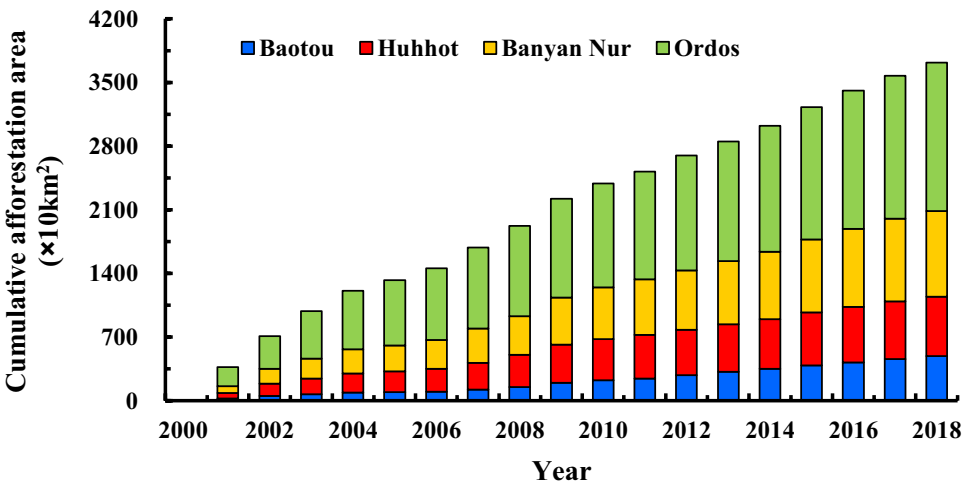

Fig. 13 Cumulative afforestation area from 2001 to 2018

TNSP", "the NFCP", and "the GTGP". These projects effectively controlled the area of desertification and improved the regional vegetation coverage (Wang et al. 2010; Ma et al. 2019). In addition, in the HTID, the improvement of vegetation in the irrigation area may benefit from the implementation of the water-saving project of irrigation area since 1998 (Qu et al. 2015) The irrigation area saved water resources by 3×10^8 m^3 in 2012 compared with in 1999 (Qu et al. 2015). At the same time, the implementation of drainage engineering has significantly reduced the groundwater level and mitigated soil salinization. Compared with in 2001, the effective irrigation area and the total sown area of crops in Banyan Nur in 2018 increased by 794.60 km^2 and 3524.90 km^2, respectively. The implementation of these projects greatly mitigated soil salinization, improved agricultural production, and increased surface vegetation coverage.

Conclusions

We used geographic detectors to ascertain the contributions of detection factors to vegetation coverage change in the YRB (IMS) and the four sub-regions. The vegetation landscape was composed of small patches with a high degree of fragmentation. However, patch connectivity has increased in recent years. In the YRB (IMS), the overall vegetation coverage displayed a slightly fluctuating upward trend from 2000 to 2018. The weather condition was getting warmer and wetter gradually. And the relative humidity and sunshine duration were decreasing. The spatial pattern of vegetation coverage change and climate change showed obvious spatial heterogeneity. The decreasing of grassland area and the increasing of built-up land area were noticeable changes of land use. Annual precipitation change was a key driving factor to vegetation coverage change in the whole area, and the interaction between land use change and annual precipitation change demonstrated the largest explanatory power to vegetation coverage change. The main human activities affecting vegetation coverage in the sub-regions were different.

Agricultural development highly relies on water sources in arid areas. To some extent, the development of irrigated agriculture causes the waste of water resources, and unreasonable irrigation leads to soil salinization. Therefore, the government should pay more attention to the drainage facilities and irrigation projects in irrigation agriculture developing. In arid and semi-arid regions, vegetation restoration should pay attention to find scientific and reasonable methods and step by step. Effectively improve the ecological environment and avoid the waste of water resources. Urban expansion makes economic development. At the same time, urban expansion causes water pollution and leads to a lot of ecological problems. Therefore, urban expansion should fully consider the ecological environment carrying capacity.

Author contribution XD: investigation, methodology, and writing-original draft. SH: Conceptualization, investigation, and writing-review and editing. CZ: Conceptualization, Supervision and project administration. All authors have read and agreed to the published version of the manuscript.

Funding This research was supported by the Major Science and Technology Projects of Inner Mongolia Autonomous Region [grant number 2020ZD0009] and the National Natural Science Foundation of China [grant number 41971232].

Data availability Not applicable.

Declarations

Ethics approval and consent to participate Not applicable.

Consent for publication Not applicable.

Competing interests The authors declare no competing interests.

References

Bai XL, Ji SX, Wang LX, Chen ZX, Chang XL (2019) Response of change trend of vegetation productivity to land use conversion in Ten Tributaries Basin of Ordos. J Nat Resour 34(06):1186–1195. https://doi.org/10.31497/zrzyxb.20190605

Chen XJ, Mo XG, Hu S, Liu SX (2017) Contributions of climate change and human activities to ET and GPP trends over North China plain from 2000 to 2014. J Geogr Sci 27(6):661–680. https://doi.org/10.1007/s11442-017-1399-z

Chen YZ, Chen LY, Cheng Y, Ju WM, Chen HYH, Ruan HH (2020) Afforestation promotes the enhancement of forest LAI and NPP in China. For Ecol Manage 462:117990. https://doi.org/10.1016/j.foreco.2020.117990

Chuai XW, Huang XJ, Wang WJ, Bao G (2013) NDVI, temperature and precipitation changes and their relationships with different vegetation types during 1998–2007 in Inner Mongolia, China. Int J Climatol 33(7):1696–1706. https://doi.org/10.1002/joc.3543

Daham A, Han DW, Rico-Ramirez M, Marsh A (2018) Analysis of NDVI variability in response to precipitation and air temperature in different regions of Iraq, using MODIS vegetation indices. Environ Earth Sci 77(10):389. https://doi.org/10.1007/s12665-018-7560-x

Du JQ, Fu Q, Fang SF, Wu JH, He P, Quan ZJ (2019) Effects of rapid urbanization on vegetation cover in the metropolises of China over the last four decades. Ecol Indic 107:105458. https://doi.org/10.1016/j.ecolind.2019.105458

Feng DR, Wang JM, Fu MC, Liu GC, Zhang M, Tang RB (2019) Spatiotemporal variation and influencing factors of vegetation cover in the ecologically fragile areas of China from 2000 to 2015: a case study in Shaanxi Province. Environ Sci Pollut Res 26(28):28977–28992. https://doi.org/10.1007/s11356-019-06096-9

Gao YD, Qiao RR, Ji SX, Bai XL, Wang LX, Chang XL (2021) Changes and driving factors of crops planting structure in Hetao Irrigation Region in Inner Mongolia. J Desert Res

41(03):110–117. https://doi.org/10.7522/j.issn.1000-694X.2020.00123
Gutman G, Ignatov A (1998) The derivation of the green vegetation fraction from NOAA/AVHRR data for use in numerical weather prediction models. Int J Remote Sen 19(8):1533–1543. https://doi.org/10.1080/014311698215333
Han JJ, Wang JP, Chen L, Xiang JY, Ling ZY, Li QK, Wang EL (2021) Driving factors of desertification in Qaidam Basin, China: an 18-year analysis using the geographic detector model. Ecol Indic 124:107404. https://doi.org/10.1016/j.ecolind.2021.107404
Hao RF, Yu DY, Liu YP, Liu Y, Qiao JM, Wang X, Du JS (2017) Impacts of changes in climate and landscape pattern on ecosystem services. Sci Total Environ 579:718–728. https://doi.org/10.1016/j.scitotenv.2016.11.036
Hao J, Xu GY, Luo L, Zhang Z, Yang HL, Li HY (2020) Quantifying the relative contribution of natural and human factors to vegetation coverage variation in coastal wetlands in China. Catena 188:104429. https://doi.org/10.1016/j.catena.2019.104429
Hilker T, Natsagdorj E, Waring RH, Lyapustin A, Wang YJ (2014) Satellite observed widespread decline in Mongolian grasslands largely due to overgrazing. Glob Change Biol 20(2):418–428. https://doi.org/10.1111/gcb.12365
Holben BN (1986) Characteristics of maximum-value composite images from temporal-AVHRR data. Int J Remote Sens 7(11):1417–1434. https://doi.org/10.1080/01431168608948945
Hu MM, Xia BC (2019) A significant increase in the normalized difference vegetation index during the rapid economic development in the Pearl River Delta of China. Land Degrad Dev 30(4):359–370. https://doi.org/10.1002/ldr.3221
Hua WJ, Chen HS, Zhou LM, Xie ZH, Qin MH, Li X, Ma HD, Huang QH, Sun SL (2017) Observational quantification of climatic and human influences on vegetation greening in China. Remote Sens 9(5):425. https://doi.org/10.3390/rs9050425
Huang X, Ma L, Liu YX, Wang JR, Liu DH (2016) Variations and periodic symmetry of temperature and precipitation in Inner Mongolia Section of the Yellow River basin during 1951–2012. J Nat Resour 31(06):1027–1040. https://doi.org/10.11849/zrzyxb.20150045
Huang K, Zhang YJ, Zhu JT, Liu YJ, Zu JX, Zhang J (2016b) The influences of climate change and human activities on vegetation dynamics in the Qinghai-Tibet Plateau. Remote Sens 8(10):876. https://doi.org/10.3390/rs8100876
Jiang WG, Yuan LH, Wang WJ, Cao R, Zhang YF, Shen WM (2015) Spatio-temporal analysis of vegetation variation in the yellow river basin. Ecol Indic 51:117–126. https://doi.org/10.1016/j.ecolind.2014.07.031
Jiang LG, Liu Y, Wu S, Yang C (2021) Analyzing ecological environment change and associated driving factors in China based on NDVI time series data. Ecol Indic 129:107933. https://doi.org/10.1016/j.ecolind.2021.107933
Kendall MG (1975) Rank correlation methods. Griffin, London
Lawley V, Lewis M, Clarke K, Ostendorf B (2016) Site-based and remote sensing methods for monitoring indicators of vegetation condition: an Australian review. Ecol Indic 60:1273–1283. https://doi.org/10.1016/j.ecolind.2015.03.021
Li CH, Yang ZF (2004) Spatio-temporal changes of NDVI and their relations with precipitation and runoff in the Yellow River Basin. Geogr Res 23:753–759
Li JJ, Peng SZ, Li Z (2017) Detecting and attributing vegetation changes on China's Loess Plateau. Agric for Meteorol 247:260–270. https://doi.org/10.1016/j.agrformet.2017.08.005
Li Y, Xie ZX, Qin YC, Zheng ZC (2019) Responses of the Yellow River basin vegetation: climate change. Int J Clim Chang Strateg Manag 11(4):483–498. https://doi.org/10.1108/IJCCSM-08-2018-0064
Liu YL, Lei HM (2015) Responses of natural vegetation dynamics to climate drivers in China from 1982 to 2011. Remote Sens 7(8):10243–10268. https://doi.org/10.3390/rs70810243
Liu XX, Tian ZX, Zhang AB, Zhao AZ, Liu HX (2019) Impacts of climate on spatiotemporal variations in vegetation NDVI from 1982–2015 in Inner Mongolia. China Sustain 11(3):768. https://doi.org/10.3390/su11030768
Ma YH, Fan SY, Zhou LH, Dong ZY, Zhang KC, Feng JM (2007) The temporal change of driving factors during the course of land desertification in arid region of North China: the case of Minqin County. Environ Geol 51(6):999–1008. https://doi.org/10.1007/s00254-006-0369-z
Ma QM, Long YP, Jia XP, Wang HB, Li YS (2019) Vegetation response to climatic variation and human activities to climatic variation and human activities on the Ordos Plateau from 2000 to 2016. Environ Earth Sci 78(24):709. https://doi.org/10.1007/s12665-019-8732-z
Mann HB (1945) Nonparametric tests against trend. Econometrica 13(3):245–259. https://doi.org/10.2307/1907187
Miao CY, Yang L, Chen XH, Gao Y (2012) The vegetation cover dynamics (1982–2006) in different erosion regions of the Yellow River Basin, China. Land Degrad Dev 23(1):62–71. https://doi.org/10.1002/ldr.1050
Mu SJ, Chen YZ, Li JL, Ju WM, Odeh IOA, Zou XL (2013) Grassland dynamics in response to climate change and human activities in Inner Mongolia, China between 1985 and 2009. Rangeland J 35(3):315–329. https://doi.org/10.1071/RJ12042
Peng SS, Piao SL, Ciais P, Myneni RB, Chen AP, Chevallier F, Dolman AJ, Janssens IA, Penuelas J, Zhang GX, Vicca S, Wan SQ, Wang SP, Zeng H (2013) Asymmetric effects of daytime and night-time warming on Northern Hemisphere vegetation. Nature 501(7465):88–92. https://doi.org/10.1038/nature12434
Peng WF, Kuang TT, Tao S (2019) Quantifying influences of natural factors on vegetation NDVI changes based on geographical detector in Sichuan, western China. J Clean Prod 233:353–367. https://doi.org/10.1016/j.jclepro.2019.05.355
Potter CS, Brooks V (1998) Global analysis of empirical relations between annual climate and seasonality of NDVI. Int J Remote Sens 19(15):2921–2948. https://doi.org/10.1080/014311698214352
Qu ZY, Yang X, Huang YJ (2015) Analysis and assessment of water-saving project of Hetao Irrigation District in Inner Mongolia. Trans Chin Soc Agric Mach 46(04):70-76+112. https://doi.org/10.6041/j.issn.1000-1298.2015.04.012
Qu S, Wang LC, Lin AW, Zhou HJ, Yuan MX (2018) What drives the vegetation restoration in Yangtze River basin, China: climate change or anthropogenic factors? Ecol Indic 90:438–450. https://doi.org/10.1016/j.ecolind.2018.03.029
Sen PK (1968) Estimates of the regression coefficient based on Kendall's tau. J Am Stat Assoc 63:1379–1389. https://doi.org/10.1080/01621459.1968.10480934
Shen Q, Gao GY, Han F, Xiao FY, Ma Y, Wang S, Fu BJ (2018) Quantifying the effects of human activities and climate variability on vegetation cover change in a hyper-arid endorheic basin. Land Degrad Dev 29(10):3294–3304. https://doi.org/10.1002/ldr.3085
Stow D, Petersen A, Hope A, Engstrom R, Coulter L (2007) Greenness trends of Arctic tundra vegetation in the 1990s: comparison of two NDVI data sets from NOAA AVHRR systems. Int J Remote Sens 28(21):4807–4822. https://doi.org/10.1080/01431160701264284
Sun R, Liu CM, Zhu QJ (2001) Relationship between the fractional vegetation cover change and rainfall in the Yellow River Basin. Acta Geogr Sin 56(6):667–672
Tian HJ, Cao CX, Chen W, Bao SN, Yang B, Myneni RB (2015) Response of vegetation activity dynamic to climatic change and ecological restoration programs in Inner Mongolia from 2000 to 2012. Ecol Eng 82:276–289. https://doi.org/10.1016/j.ecoleng.2015.04.098
Tian F, Liu LZ, Yang JH, Wu JJ (2021) Vegetation greening in more than 94% of the Yellow River Basin (YRB) region in China during the 21st century caused jointly by warming and anthropogenic

activities. Ecol Indic 125:107479. https://doi.org/10.1016/j.ecolind.2021.107479
Vereecken H, Kollet S, Simmer C (2010) Patterns in soil–vegetation–atmosphere systems: monitoring, modeling, and data assimilation. Vadose Zone J 9(4):821–827. https://doi.org/10.2136/vzj2010.0122
Wang XM, Zhang CX, Hasi E, Dong ZB (2010) Has the Three Norths Forest Shelterbelt program solved the desertification and dust storm problems in arid and semiarid China? J Arid Environ 74(1):13–22. https://doi.org/10.1016/j.jaridenv.2009.08.001
Wang J, Wang KL, Zhang MY, Zhang CH (2015) Impacts of climate change and human activities on vegetation cover in hilly southern China. Ecol Eng 81:451–461. https://doi.org/10.1016/j.ecoleng.2015.04.022
Wang JF, Zhang TL, Fu BJ (2016) A measure of spatial stratified heterogeneity. Ecol Indic 67:250–256. https://doi.org/10.1016/j.ecolind.2016.02.052
Wang JF, Xu CD (2017) Geodetector: principle and prospective. Acta Geogr Sin 72(01):116–134. https://doi.org/10.11821/dlxb201701010
Wang LX, Cai MY, Bai XL, Ji SX, Jia B, Feng XW, Chang XL (2021) Estimation of irrigation area in Hetao Irrigation District based on MODIS analysis. J Inn Mong Norm Univ Nat Sci Ed 50(01):44–52. https://doi.org/10.3969/j.issn.1001-8735.2021.01.007
Wen ZF, Wu SJ, Chen JL, Lu MQ (2017) NDVI indicated long-term interannual changes in vegetation activities and their responses to climatic and anthropogenic factors in the Three Gorges Reservoir Region. China Sci Total Environ 574:947–959. https://doi.org/10.1016/j.scitotenv.2016.09.049
Wu ZT, Wu JJ, Liu JH, He B, Lei TJ, Wang QF (2013) Increasing terrestrial vegetation activity of ecological restoration program in the Beijing-Tianjin Sand Source Region of China. Ecol Eng 52:37–50. https://doi.org/10.1016/j.ecoleng.2012.12.040
Wu YJ, Dong SC, Huang HS, Zhai J, Li Y, Huang DX (2018) Quantifying uban land expansion dynamics through improved land management institution model: application in Ningxia-Inner Mongolia, China. Land Use Pol 78:386–396. https://doi.org/10.1016/j.landusepol.2018.06.018
Xu G, Zhang HF, Chen BZ, Zhang HR, Innes JL, Wang GY, Yan JW, Zheng YH, Zhu ZC, Myneni RB (2014) Changes in vegetation growth dynamics and relations with climate over China's Landmass from 1982 to 2011. Remote Sens 6(4):3263–3283. https://doi.org/10.3390/rs6043263
Xie BN, Jia XX, Qin ZF, Shen J, Chang QR (2016) Vegetation dynamics and climate change on the Loess Plateau, China: 1982–2011. Reg Envir Chang 16(6):1583–1594. https://doi.org/10.1007/s10113-015-0881-3
Yan XX, Li J, Shao Y, Hu ZQ, Yang Z, Yin SQ, Cui LY (2020) Driving forces of grassland vegetation changes in Chen Barag Banner. Inner Mongolia Gisci Remote Sens 57(6):753–759. https://doi.org/10.1080/15481603.2020.1794395
Yang Z, Shen YY, Jiang HW, Feng FS, Dong QL (2021) Assessment of the environment changes in arid and semiarid areas using long time-series Landsat images. Environ Sci Pollut Res 28(37):52147–52156. https://doi.org/10.1007/s11356-021-14417-0
You NS, Meng JJ, Sun MT (2019) Spatio-temporal change of NDVI and its relationship with climate in the upper and middle reaches of Heihe River Basin from 2000 to 2015. Acta Sci Nat Univ Pekin 55:171–181. https://doi.org/10.13209/j.0479-8023.2018.075
Yuan J, Xu YP, Xiang J, Wu L, Wang DQ (2019) Spatiotemporal variation of vegetation coverage and its associated influence factor analysis in the Yangtze River Delta, eastern China. Environ Sci Pollut Res 26(32):32866–32879. https://doi.org/10.1007/s11356-019-06378-2
Zhang Y, Peng CH, Li WZ, Tian LX, Zhu QA, Chen H, Fang XQ, Zhang GL, Liu GB, Mu XM, Li ZB, Li SQ, Yang YZ, Wang J, Xiao XM (2016) Multiple afforestation programs accelerate the greenness in the 'Three North' region of China from 1982 to 2013. Ecol Indic 61:404–412. https://doi.org/10.1016/j.ecolind.2015.09.041
Zhang XL, Huang XR (2019) Human disturbance caused stronger influence on global vegetation change than climate change. PeerJ 7:e7763. https://doi.org/10.7717/peerj.7763
Zhang W, Wang L C, Xiang F F, Qin W M, Jiang W X (2020a) Vegetation dynamics and the relations with climate change at multiple time scales in the Yangtze River and Yellow River Basin, China. Ecol. Indic., 110https://doi.org/10.1016/j.ecolind.2019.105892
Zhang M, Wang JM, Li SJ, Feng DR, Cao EL (2020b) Dynamic changes in landscape pattern in a large-scale opencast coal mine area from 1986 to 2015: a complex network approach. CATENA 194:104738. https://doi.org/10.1016/j.catena.2020.104738
Zhao L, Dai AG, Dong B (2018) Changes in global vegetation activity and its driving factors during 1982–2013. Agric for Meteorol 249:198–209. https://doi.org/10.1016/j.agrformet.2017.11.013
Zhou HJ, Van Rompaey A, Wang JA (2009) Detecting the impact of the "Grain for Green" program on the mean annual vegetation cover in the Shaanxi province, China using SPOT-VGT NDVI data. Land Use Pol 26(4):954–960. https://doi.org/10.1016/j.landusepol.2008.11.006
Zhu LJ, Meng JJ, Zhu LK (2020) Applying geodetector to disentangle the contributions of natural and anthropogenic factors to NDVI variations in the middle reaches of the Heihe River Basin. Ecol Indic 117:106545. https://doi.org/10.1016/j.ecolind.2020.106545